

Efficiency of optically pumping a quantum battery and a two-stroke heat engine

Tiago F. F. Santos^{1,*} and Marcelo F. Santos¹

¹*Instituto de Física, Universidade Federal do Rio de Janeiro,
CP68528, Rio de Janeiro, Rio de Janeiro 21941-972, Brazil*

(Dated: August 5, 2022)

In this work, we study the efficiency of charging a quantum battery through optical pumping. The battery consists of a qutrit and it is connected to a natural thermal reservoir and an external coherent drive in the limit where its upper energy level can be adiabatically eliminated from the dynamics. In this scenario, the drive plus spontaneous emission optically pumps the intermediate energy level of the qutrit and the battery can be understood as being charged by an effective higher temperature reservoir that takes it out of equilibrium with the natural reservoir and stores useful energy in it. We also analyse the efficiency of using this battery and charging scheme as the work fluid of a two-stroke thermal machine.

I. INTRODUCTION

The growing interest in quantum technologies and the continuous miniaturization of current devices has made it essential to understand the thermodynamics laws on micro and nano-scales. It has also led to a growing research interest in devices where microscopic media are used as the work fluid of heat engines or as energy storing quantum batteries.

A quantum heat engine is a machine whose work fluid is a quantum system operating in or out of equilibrium. In that sense, any quantum system coherently and incoherently exchanging energy with its environment can be interpreted as such a machine. In fact, the first quantum dynamics viewed as a quantum heat engine was a three-level maser [1]. Since then, many different analogues of classical heat engines operating in equivalents Carnot and Otto cycles have been studied [2–18], as well as many other more general models [18–32]. In most cases, the main goal is to define the efficiency and output power of the machines, their particular regimes of operations and if they present some quantum advantage when compared to their classical counterparts, when there is one.

In parallel to that, another relevant energetic problem related to the development of new quantum technologies concerns the efficiency and input power of the charging of quantum batteries [33], namely quantum systems that can store energy to be later extracted as work. The charging of quantum batteries has been studied both for unitary dynamics [34–41] as well as for incoherent processes [42–52]. In most cases, the target of investigation has been the enhancement of input power due to quantum properties such as coherence and correlation [53–60], whereas in [42, 44, 61–64] the authors also analyse the energetic efficiency of the charging process. None of them, however, includes in the calculation of the charging efficiency the eventual cost to produce anomalous energy sources such as structured or engineered reservoirs or “classical” drives.

In this work, we study the efficiency and input power of the charging of a particular quantum battery through a process known as optical pumping. The battery consists of a qutrit that is coupled to an external work drive and to a standard thermal reservoir in a typical optical pumping setup (see Fig. 1). We assume that the qutrit is initially in thermal equilibrium with the reservoir and it is driven out of equilibrium by the coherent external source, so that useful energy is stored in it. We analyze the efficiency and the stored power in this process taking into consideration the energy transferred by the external “classical” source as well as that exchanged with the thermal reservoir, in the limit where the upper energy level of the qutrit can be adiabatically eliminated from the dynamics [65, 66]. In the sequence, we use this battery as the quantum work fluid of a two-stroke thermal machine and study its efficiency and output power in the same regime. The engine includes a fourth level and operates a cycle where energy is stored through the optical pumping and extracted by means of an unitary transformation.

The paper is organized as follows. In Sec. II we revisit the theory of quantum open system dynamics and thermodynamics and present our models of the quantum battery and the two-stroke quantum heat engine. We also show some algebraic results for particular regimes of operation of the machine. In Sec. III we show and analyze the numerical results for both setups. Finally, in Sec. IV we summarize and comment on the results and discuss possible future developments. Details of the calculations are reported in the Appendix

II. THEORETICAL BACKGROUND

A. Open quantum system dynamics and thermodynamics

Here we will assume that the interaction between the quantum system and the thermal reservoir is Markovian so that the dynamics is ruled by a master equation in the

* Corresponding author: tffs@pos.if.ufrj.br

Lindblad form [67] ($\hbar = k_B = 1$ in the following):

$$\dot{\rho} = -i[H(t), \rho] + \mathcal{L}(\rho). \quad (1)$$

The first term on the right side accounts for the unitary part of the dynamics. The Hamiltonian reads $H(t) = H_0 + V(t)$, where H_0 is the free Hamiltonian of the system (e.g. non-degenerate three or four-level atoms) and $V(t)$ accounts for its coupling with external coherent sources (e.g. laser fields). The second term represents the non-unitary part of the dynamics, $\mathcal{L}(\rho)$, given by

$$\mathcal{L}(\rho) = \sum_j L_j(\rho) = \sum_j \Gamma_j \left[J_j \rho J_j^\dagger - \frac{1}{2} \{J_j^\dagger J_j, \rho\} \right], \quad (2)$$

where $\{A, B\} = AB + BA$, Γ_j are the incoherent energy exchange rates and J_j are the corresponding energy jump operators in the system. In this scenario and defining the internal energy of the system at time t as the expectation value of its total energy, $U(t) = \text{Tr}\{\rho(t)H(t)\}$, R. Alicki [19] has defined the work, W , and the heat, Q , exchanged between the system and the reservoirs respectively by

$$W = \int_{t_0}^t dt' \text{Tr}\{\rho(t') \dot{H}(t')\} \quad (3)$$

and

$$Q = \int_{t_0}^t dt' \text{Tr}\{\dot{\rho}(t') H(t')\} = \int_{t_0}^t dt' \text{Tr}\{\mathcal{L}[\rho(t')] H(t')\}. \quad (4)$$

Note that these definitions automatically satisfy the first law of thermodynamics. Even though there has been a long discussion about the definitions of work and heat in quantum thermodynamics [68–71], for all the purposes of this paper, Alicki's are satisfactory.

In order to analyze the efficiency of the charging of our battery we need to compute its non-equilibrium Helmholtz free energy, $F(t) = U(t) - TS(t)$, where T is the temperature of the reservoir in which the system is embedded and $S(t)$ is the von Neumann entropy of the system, $S(t) = -\text{Tr}\{\rho(t) \ln[\rho(t)]\}$. We also need to remember that in an isothermal and generally irreversible process, the maximum amount of work, W_{ext} , that can be extracted or stored in the battery is at most equal to a decrease or increase in its Helmholtz free energy, $|W_{ext}| \leq |\Delta F|$, where the equality holds for reversible processes.

B. Quantum battery model

We consider a quantum battery (Fig. 1) that consists of a qutrit of levels $|g\rangle$, $|i\rangle$ and $|m\rangle$ ($E_g = 0 < E_i < E_m$) connected to an external work drive, $V_{in}(t) = \Omega (\sigma_{gm} e^{i\omega_f t} + \sigma_{mg} e^{-i\omega_f t})$ ($\sigma_{kl} \equiv |k\rangle\langle l|$) that couples levels $|g\rangle$ and $|m\rangle$ and injects energy into the system, and

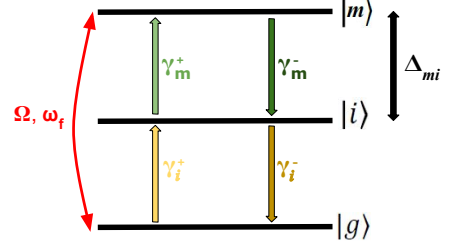


FIG. 1. A three-level system in cascade configuration scheme. The transitions between the energy levels are induced by the coupling of the system to a thermal reservoir and to an external work drive that injects energy into the system. $\Delta_{mi} = E_m - E_i$.

to a thermal reservoir of finite temperature T that generates a Markovian incoherent energy exchange with the system. The dynamics of the battery is given by Eqs. 1 and 2 where $\mathcal{L}(\rho)$ is decomposed in the following terms:

$$\begin{aligned} \mathcal{L}_{\gamma_m}[\rho(t)] &= \frac{\gamma_m^+}{2} (2\sigma_{mi}\rho(t)\sigma_{im} - \{\sigma_{ii}, \rho(t)\}) \\ &\quad + \frac{\gamma_m^-}{2} (2\sigma_{im}\rho(t)\sigma_{mi} - \{\sigma_{mm}, \rho(t)\}), \end{aligned} \quad (5)$$

where $\gamma_m^+ = \gamma_0^m \bar{n}_m$, $\gamma_m^- = \gamma_0^m (\bar{n}_m + 1)$ and $\bar{n}_m = \left(e^{\frac{E_m - E_i}{T}} - 1\right)^{-1}$, and

$$\begin{aligned} \mathcal{L}_{\gamma_i}[\rho(t)] &= \frac{\gamma_i^+}{2} (2\sigma_{ig}\rho(t)\sigma_{gi} - \{\sigma_{gg}, \rho(t)\}) \\ &\quad + \frac{\gamma_i^-}{2} (2\sigma_{gi}\rho(t)\sigma_{ig} - \{\sigma_{ii}, \rho(t)\}), \end{aligned} \quad (6)$$

where $\gamma_i^+ = \gamma_0^i \bar{n}_i$, $\gamma_i^- = \gamma_0^i (\bar{n}_i + 1)$ and $\bar{n}_i = \left(e^{\frac{E_i - E_g}{T}} - 1\right)^{-1}$. Note that we consider that the reservoir does not directly couples levels $|m\rangle$ and $|g\rangle$ or that, if it does, this coupling is very weak when compared to the others (two approximations commonly found in quantum optical systems).

We assume that the system is in contact with the natural reservoir at temperature T and, thus, it is initially prepared in a Gibbs state, $\rho(0) = e^{-\beta H_0}/Z$, where $H_0 = \omega_j |E_j\rangle\langle E_j|$, $\beta = 1/T$ and $Z = \text{Tr}(e^{-\beta H_0})$ is the partition function. Turning on $V_{in}(t)$ evolves the system into a non-equilibrium energy storing steady state, ρ_{NESS} , whose free energy is larger than that of $\rho(0)$ (see the Appendix for a detailed calculation of the dynamics). The efficiency of this process is given by $\eta_{pump} = \frac{\Delta F}{E_{in}}$, and its input power by $\mathcal{P}_{pump} = \frac{\Delta F}{\tau}$, where E_{in} is the total energy injected into the system, τ is the time it takes for the system to reach ρ_{NESS} from the initial Gibbs state $\rho(0)$, and $\Delta F = F_{NESS} - F(0)$ is the variation

of Helmholtz free energy. There are two possible energy sources for the process: the external drive and the thermal reservoir. The first will always inject energy in the battery whereas the latter may or may not do so, depending on the parameters. In order to compute the total amount of injected energy, E_{in} , we need to consider

$$E_{in} = \text{Max}\{W_{in}, W_{in} + Q_{\gamma_m}, W_{in} + Q_{\gamma_i}, W_{in} + Q\}, \quad (7)$$

where W_{in} is the work done by the external source and Q_k the heat injected by reservoir k . Taking $V_{in}(t)$ into consideration, the injected work is given by

$$W_{in} = i\Omega\omega_f \int_0^\tau dt [\varrho_{mg}(t) - \varrho_{gm}(t)], \quad (8)$$

where $\varrho_{gm} = \langle g|e^{iH_0 t}\rho e^{-iH_0 t}|m\rangle$, whereas the heat components of the energy exchange are given by

$$Q_{\gamma_m} = -\Omega \frac{\gamma_m^-}{2} \int_0^\tau dt [\varrho_{mg}(t) + \varrho_{gm}(t)] \\ + (\omega_m - \omega_i) \int_0^\tau dt [\gamma_m^+ \varrho_{ii}(t) - \gamma_m^- \varrho_{mm}(t)], \quad (9)$$

between levels $|m\rangle$ and $|i\rangle$, and

$$Q_{\gamma_i} = -\Omega \frac{\gamma_i^+}{2} \int_0^\tau dt [\varrho_{mg}(t) + \varrho_{gm}(t)] \\ + \omega_i \int_0^\tau dt [\gamma_i^+ \varrho_{gg}(t) - \gamma_i^- \varrho_{ii}(t)], \quad (10)$$

between levels $|i\rangle$ and $|g\rangle$. $Q = Q_{\gamma_m} + Q_{\gamma_i}$ is the total heat exchange.

In this work, we are interested in the scenario where we can adiabatically eliminate level $|m\rangle$ from the dynamics. This limit is achieved if we consider that the decay rate from level $|m\rangle$ to $|i\rangle$ is much larger than the other rates involved in the dynamics, $\gamma_m^- \gg \gamma_m^+, \gamma_i^\pm, \Omega$. Under these conditions, the population of level $|m\rangle$ becomes approximately stationary and very small when compared to the others, in a time scale that is much smaller than the effective changes experienced by the battery. In this case, the combination of the external work drive with spontaneous emission optically pumps level $|i\rangle$, i.e. population is effectively and incoherently transferred straight from level $|g\rangle$ to level $|i\rangle$, and Eq. (8) reads

$$W_{in} = p\omega_f \gamma_m^- \int_0^\tau dt \varrho_{gg}(t), \quad (11)$$

where

$$p = \frac{4\Omega^2}{\gamma_m^{-2} + 4\Delta\omega^2} \quad (12)$$

is the pumping rate. For fixed values of Ω and γ_m^- , p is maximized when $\Delta\omega = \omega_f - \omega_m = 0$, i.e., when the laser drives the $|g\rangle \rightarrow |m\rangle$ transition resonantly. As for the exchanged heat, Eqs. (9) and (10) read

$$Q_{\gamma_m} \approx p\gamma_m^- (\omega_i - \omega_f) \int_0^\tau dt \varrho_{gg}(t) \quad (13)$$

and

$$Q_{\gamma_i} = -p\gamma_i^+ \Delta\omega \int_0^\tau dt \varrho_{gg}(t) \\ + \omega_i \int_0^\tau dt (\gamma_i^+ \varrho_{gg}(t) - \gamma_i^- \varrho_{ii}(t)). \quad (14)$$

These are the equations ultimately used to compute η_{pump} and $\mathcal{P}_{\text{pump}}$. Before advancing to the next section it is worth noting that the optical pumping plus the natural reservoir can be seen as an effective higher temperature reservoir acting on the $\{|g\rangle, |i\rangle\}$ transition, given that the adiabatic elimination of level $|m\rangle$ produces an effective dynamics in the system that corresponds to an extra term of the type $\mathcal{L}_p(\rho) = p\gamma_m^- (2\sigma_{ig}\rho\sigma_{gi} - \{\sigma_{gg}, \rho\})$. This term unbalances the natural ratio $\frac{\gamma_i^-}{\gamma_i^+}$ and produces an effective higher temperature $T_H = \frac{\hbar\omega_i}{k_B \ln(\frac{\gamma_i^-}{p\gamma_m^- + \gamma_i^+})}$ in the subspace [72–74].

C. Quantum heat engine model

The proposed quantum heat engine is based on the version developed in [43] of a two-stage machine. The first stage uses an effective temperature difference to recharge the work fluid and the second stage, a unitary operation to extract work from it. Here, we will consider the battery described in the last section as the work fluid of the machine.

The operation of the machine requires introducing a fourth level $|e\rangle$ into the system, whose energy E_e lies in between those of levels $|g\rangle$ and $|i\rangle$ (see Fig. 2) - $E_g = 0 < E_e < E_i < E_m$. The $|g\rangle \rightarrow |e\rangle$ transition is in contact only with the natural reservoir at temperature T . When level $|m\rangle$ is adiabatically eliminated from the dynamics, the optical pumping of level $|i\rangle$, produced by $V_{in}(t)$, eventually inverts the population in the subspace $\{|e\rangle, |i\rangle\}$. This is equivalent to say that the machine operates under a temperature difference $T_H - T$ where T_H (T) affects the $\{|g\rangle, |i\rangle\}$ ($\{|g\rangle, |e\rangle\}$) subspace. This difference in temperature establishes a heat flux through the system and if heat flows through the system for a long enough time it eventually produces states that are diagonal in the H_0 eigenbasis and given by $\rho_{OSS} = \sum_k r_k \sigma_{kk}$ ($k = g, e, i$), with $r_g > r_i > r_e$. Because the machine operates in closed cycles, we refer to these states as “Operational Steady States”, hence the label OSS. Such states have positive ergotropy [75], $\mathcal{E} = (E_i - E_e)(r_i - r_e)$, meaning they store energy that can be extracted in the form of work by unitary operations. The largest population difference (largest value of ergotropy) is achieved asymptotically and corresponds to the most amount of energy that can be stored by the recharging stage. This particular OSS is called the “Non-equilibrium steady state (NESS)”, from now on labelled ρ_{NESS} . Previous works [43, 77] have shown, however,

that NESS is not necessarily the best regime for the operation of the machine. In general, intermediate charging times will be used, generating ρ_{OSS} that carry less ergotropy but are much faster to recharge. The faster recharging time, from now on referred to as τ_r , increases both the output power that depends on the inverse of the total duration of the cycle as well as the efficiency since less heat is lost to the reservoirs. To each τ_r there corresponds a particular state ρ_{OSS} .

The second stage of the machine, called the discharging stage, corresponds to a swap of the $|e\rangle$ and $|i\rangle$ populations, for the class of OSS here analyzed. Physically, such swap can be implemented by turning on a second external source, $V_{ext}(t) = \epsilon (\sigma_{ei}e^{i(\omega_i-\omega_e)t} + \sigma_{ie}e^{-i(\omega_i-\omega_e)t})$ for a finite time $\tau_d = \frac{\pi}{2\epsilon}$, in what is known as a $\pi/2$ pulse. This pulse takes ρ_{OSS} into a corresponding passive state [76] of the form $\rho_{OSS}(\tau_d) = r_g|g\rangle\langle g| + r_i|e\rangle\langle e| + r_e|i\rangle\langle i|$, from which it can be recharged in the next cycle. Note that, by construction, the energy gained during the recharging stage balances out the energy extracted during the discharging stage so that $\Delta U_{cycle} = 0$ in a cycle, as expected.

From the dynamical point of view, taking level $|e\rangle$ into consideration adds extra non-unitary terms to the time evolution of the machine. Once again we will consider that the natural reservoir directly couples only levels $|e\rangle$ and $|g\rangle$ but does not act (or acts very weakly) in the $|e\rangle \rightarrow |i\rangle$ transition. This approximation simplifies the calculations with no loss of generality. The new terms read

$$\begin{aligned} \mathcal{L}_{\gamma_e}[\rho(t)] = & \frac{\gamma_e^+}{2} (2\sigma_{eg}\rho(t)\sigma_{ge} - \{\sigma_{gg}, \rho(t)\}) \\ & + \frac{\gamma_e^-}{2} (2\sigma_{ge}\rho(t)\sigma_{eg} - \{\sigma_{ee}, \rho(t)\}), \end{aligned} \quad (15)$$

where $\gamma_e^+ = \gamma_0^e \bar{n}_e$, $\gamma_e^- = \gamma_0^e (\bar{n}_e + 1)$ and $\bar{n}_e = \left(e^{\frac{E_e - E_g}{T}} - 1\right)^{-1}$. Adiabatic elimination of level $|m\rangle$ also imposes $\gamma_m^- \gg \gamma_e^\pm$.

At the end of one cycle, the work done on the system, W_{in} , the work performed by the machine, W_{ext} , and the heat exchanged between the system and the thermal reservoir, Q , are, once again, computed using Eqs. 3 and 4.

In general, the energy exchanged by the machine as well as its efficiency and power output are obtained by numerically integrating in time different functions of the state of the system, similar to the ones obtained for the battery in Eqs. 8-10. However, the calculations of these quantities are significantly simpler in the ideal operational regime of the machine, derived in previous works [43, 77], that is achieved for $\tau_d \ll \tau_r$ and $\sum_j \gamma_j \tau \ll 1$. The first condition allows us to assume that the discharging stage is isentropic and isochoric, meaning that the extracted work is maximal, i.e. equal to the ergotropy stored in the system. The second condition establishes the short cycle operation, described in details in [43, 77] and characterized by a linear variation

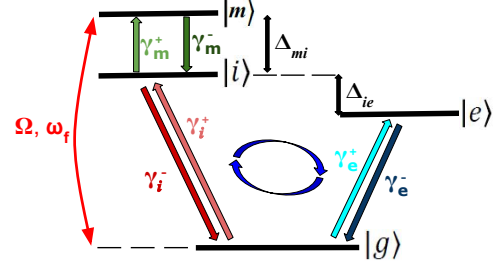


FIG. 2. A four-level system as the working fluid. The transitions between the energy levels are induced by the coupling of the system to a thermal reservoir and to an external work drive that injects energy into the system. $\Delta_{mi} = E_m - E_i$ and $\Delta_{ie} = E_i - E_e$.

with time of the thermodynamics quantities and the minimization of the heat exchanged with the reservoirs. In this regime, the work injected in the machine is given by

$$\begin{aligned} W_{in}^{SC} &= \text{Tr}[\tilde{\rho} \dot{V}_{in}(\tau)]\tau \\ &= \omega_f p \gamma_m^- \frac{\gamma_i^- + \gamma_e^-}{\kappa} \tau, \end{aligned} \quad (16)$$

where $\kappa = 2(\Gamma_i^+ + \gamma_e^+) + \gamma_i^- + \gamma_e^-$, $\Gamma_i^+ = \gamma_i^+ + p\gamma_m^-$ and p is given by Eq. (12). The heat, on its turn, can be decomposed in the following three components:

$$\begin{aligned} Q_{\gamma_e}^{SC} &= \text{Tr}\{\mathcal{L}_{\gamma_e}[\tilde{\rho}][H_0 + V_{in}(\tau)]\}\tau \\ &= \omega_e \frac{\gamma_e^+ \gamma_i^- - \Gamma_i^+ \gamma_e^-}{\kappa} \tau - p \gamma_e^+ \Delta\omega \frac{\gamma_i^- + \gamma_e^-}{\kappa} \tau, \end{aligned} \quad (17)$$

$$\begin{aligned} Q_{\gamma_i}^{SC} &= \text{Tr}\{\mathcal{L}_{\gamma_i}[\tilde{\rho}][H_0 + V_{in}(\tau)]\}\tau \\ &= \omega_i \frac{\gamma_i^+ \gamma_e^- - \gamma_i^- (\gamma_e^+ + p\gamma_m^-)}{\kappa} \tau \\ &\quad - p \gamma_i^+ \Delta\omega \frac{\gamma_i^- + \gamma_e^-}{\kappa} \tau, \end{aligned} \quad (18)$$

and

$$\begin{aligned} Q_{\gamma_m}^{SC} &= \text{Tr}\{\mathcal{L}_{\gamma_m}[\tilde{\rho}][H_0 + V_{in}(\tau)]\}\tau \\ &= (\omega_i - \omega_f) p \gamma_m^- \frac{\gamma_i^- + \gamma_e^-}{\kappa} \tau. \end{aligned} \quad (19)$$

Finally, the ergotropy stored in the system can also be algebraically computed and it is given by

$$\mathcal{E}_{SC} = (\omega_i - \omega_e) \frac{\Gamma_i^+ \gamma_e^- - \gamma_i^- \gamma_e^+}{\kappa}. \quad (20)$$

Note that all the quantities above are proportional to the cycle duration τ , and for the ergotropy to be positive it is necessary that $\frac{\Gamma_i^+}{\gamma_i^-} > \frac{\gamma_e^+}{\gamma_e^-}$. Also note that

if this condition is not fulfilled, a similar scheme can still be used as a refrigerator [78–81]. Finally note that the linear dependence on time of both ergotropy and injected energy makes both the efficiency of the short cycle, $\eta_{SC} = \mathcal{E}_{SC}/E_{in}^{SC}$ and its power output $\mathcal{P}_{SC} = \mathcal{E}_{SC}/\tau$ to be time independent, relying only on the rates of energy exchange, the temperature of the reservoir and the optical pump.

III. RESULTS

A. Quantum Battery

The first aspect to analyze regarding the charging of the battery via optical pumping is the time scales of the process. In Figs. 3 (a) and (b) we present respectively the numerical results for the pumping efficiency and the population of level $|i\rangle$ as a function of (parameterized) time. We consider a resonant pump ($\omega_f = \omega_m$) and parameters consistent with the adiabatic elimination of level $|m\rangle$ ($\gamma_m^- = 10^3\gamma_i^-$ and $\gamma_m^- = 10^4\Omega$). In Fig. 3 (a), we show that there are clearly two time scales involved in the process, as expected. The first one, much faster, concerns the coarse-graining in time required to take the adiabatic elimination of level $|m\rangle$ into consideration. Its characteristic time is of the order of $1/\gamma_m^-$ as it becomes clear in the inset where we show how the population ρ_m quickly stabilizes in time when compared to the effective dynamics of the battery dominated by γ_i^- . At $t = 0$, there is no stored power in the battery and the very first process coherently transfers population from level $|g\rangle$ to level $|m\rangle$. As the decay from $|m\rangle$ to $|i\rangle$ begins to dominate the process, the battery begins to store energy and, the closer level $|m\rangle$ gets to its asymptotic value, the more efficient this energy transference gets until the moment where almost all the energy pumped into the system is stored as population of level $|i\rangle$. That is when the efficiency reaches its peak, at which point the only wasted energy is the heat dissipated to the $|m\rangle \rightarrow |i\rangle$ reservoir and the little remaining population in level $|m\rangle$. From the efficiency point of view, this is the best operating interval for charging the battery. A glance on Fig. 3 (b), however, shows that at this time scale, the battery is far from fully charged. In fact, the population of level $|i\rangle$ is still comparable to that of level $|m\rangle$ and much smaller than its asymptotic value. The further we pump the system, the more stored power we get at the cost of lowering the efficiency of the process because, now, the system begins to dissipate heat to the $|i\rangle \rightarrow |g\rangle$ reservoir as well. This becomes clear in Fig. 4 where we plot the stored energy versus the efficiency for two different temperatures of the natural reservoir. In each curve, both plotted quantities are parameterized by the duration of the charging cycle of the battery for a fixed set of the remaining parameters. Note that the temperature does not significantly affect the process except for very short times (higher efficiencies).

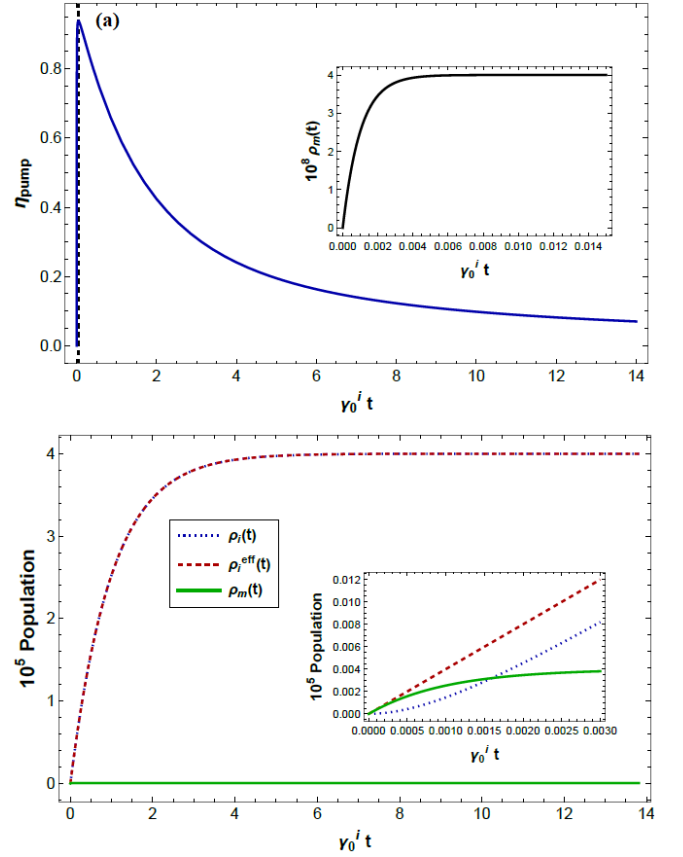


FIG. 3. We plot the pumping efficiency (Fig. (a)), η_{pump} , and the population of levels $|m\rangle$ and $|i\rangle$ (Fig. (b)) as a function of $\gamma_0^i t$ for $T = 0$ and $\omega_f = \omega_m$. In Fig. (b), ρ_i^{eff} is the population of the level $|i\rangle$ when we adiabatically eliminate level $|m\rangle$ and obtain an effective two-level system, with levels $|g\rangle$ and $|i\rangle$. Parameters: $\omega_m/\omega_i = 1.02$, $\gamma_0^m/\omega_i = 10^{-4}$, $\gamma_0^i/\omega_i = 10^{-7}$, $\Omega/\omega_i = 10^{-8}$ and $\omega_i\tau \approx 1,382 \times 10^8$. In the graphics, Bohr energies are given in units of \hbar and thermal energies in units of k_B .

Finally, we also show in Fig. 3 (b) that the chosen parameters are indeed consistent with the adiabatic elimination condition since, at the time scale of the charging of the battery, the population of level $|i\rangle$ is essentially the same taking both the full three-level or the effective two-level dynamics.

The next relevant point concerning the battery is how its charging efficiency depends on the frequency of the pumping field. In Fig. 5 we plot the efficiency of the optical pumping process as a function of the difference in energy $\Delta\omega = \omega_f - \omega_m$ between the photon coming from the external drive, of frequency ω_f , and the $|g\rangle \rightarrow |m\rangle$ transition, of frequency ω_m . This detuning is one of the main factors that affect the efficiency. If the absorbed photon has more energy than the transition it is pumping, some of its energy will be wasted into the $|i\rangle \rightarrow |m\rangle$ reservoir in the form of heat, lowering the overall efficiency of the process. This can be seen in the displayed curves where the largest efficiency

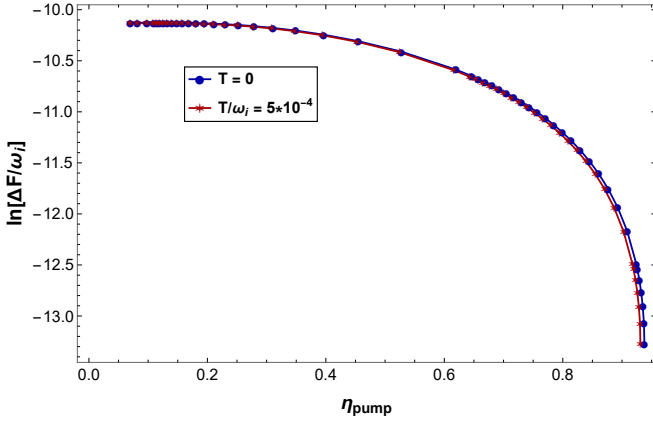


FIG. 4. Logarithm of the stored energy versus efficiency of the charging process for two temperatures. Parameters: $\omega_m/\omega_i = 1.02$, $\omega_f = \omega_m$, $\gamma_0^m/\omega_i = 10^{-4}$, $\gamma_0^i/\omega_i = 10^{-7}$, $\Omega/\omega_i = 10^{-8}$. In the graphics, Bohr energies are given in units of \hbar and thermal energies in units of k_B .

is achieved at $\omega_f = \omega_i$, no matter the temperature of the reservoir. This is the point where the energy of the absorbed photon matches that of the $|g\rangle \rightarrow |i\rangle$ transition and the least amount of energy is wasted to the reservoir. Note, however, that as long as $\Delta\omega/\omega_i \ll 1$ (which are the cases here analysed), the decay of the efficiency caused by this wasted energy is relatively small. This can be understood by calculating the approximated efficiency in the $T \rightarrow 0$ limit (see the Appendix for details). In general, the efficiency is a function of the energies and rates involved in the pumping process. However, as the temperature approaches zero, it can be approximated by $\eta_{Max} \approx 1/(\gamma_0^i\tau)$, for $\omega_f \leq \omega_i$, which is the higher efficiency achievable by the process of fully charging the battery, or to $\eta_{pump}(\Delta f_i, T = 0) \approx \left(1 - \frac{\Delta f_i}{\omega_i}\right) \eta_{Max}$, for $\Delta f_i = \omega_f - \omega_i > 0$. The dependence of η_{Max} on the inverse of the duration of the recharging process comes from the energy wasted to re-pump into level $|i\rangle$ population that is lost, at rate γ_0^i , to spontaneous emission into the $|i\rangle \rightarrow |g\rangle$ reservoir. The longer it takes for the charging of the battery the less efficient the process becomes because the battery keeps losing heat at a constant rate with marginal increase in the stored power. Also note that the pumping mechanism is always able to store useful energy in the battery. This is to be expected since no matter how small p is, it always takes the state of the battery out of thermal equilibrium.

The other mechanism that affects the efficiency is the energy fluctuation due to the natural reservoir. Its first and clearest effect comes from the fact that, for fixed values of the remaining parameters, the lower the temperature of the reservoir the higher the efficiency of the optical pumping. As we have seen, in the limit of very low T , these fluctuations do not play a significant role and the only energy waste comes from the mechanisms described above. As T increases, the relative effect of the

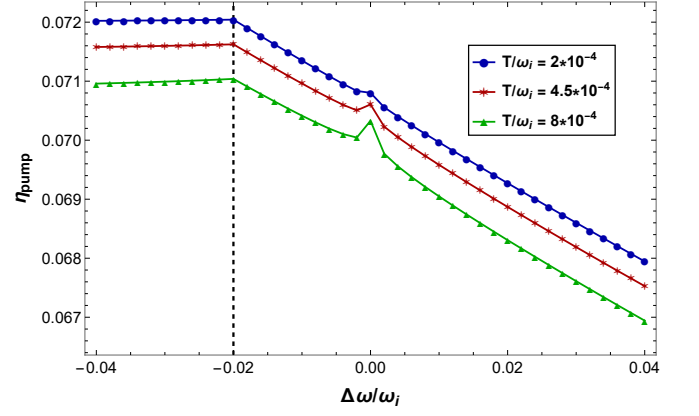


FIG. 5. We plot the pumping efficiency, η_{pump} , as a function of $\Delta\omega/\omega_i$, where $\Delta\omega = \omega_f - \omega_m$, for different temperatures. Parameters: $\Omega/\omega_i = 10^{-8}$, $\gamma_0^m/\omega_i = 10^{-4}$, $\gamma_0^i/\omega_i = 10^{-7}$ and $\omega_m/\omega_i = 1.02$.

pumping becomes less pronounced and the efficiency of the process decreases.

This mechanism, however, has two more effects. The first one is observed when the optical pumping is in resonance ($\Delta\omega = 0$), in which case the transference of energy from the external field to the battery is faster and the effect of thermal fluctuations is relatively minimized. That explains the small peak around $\omega_f = \omega_m$. Note that, as long as the conditions for the adiabatic elimination of level $|m\rangle$ hold, meaning as long as the temperature is not too high for its thermal population to become significant, the efficiency becomes approximately independent of the temperature of the reservoir at the resonance. The other effect is more subtle and slightly non-intuitive. It is observed for driving photons of energy smaller than the pumped transition, $\omega_f \leq \omega_i$. In this case, the thermal fluctuations in the $|i\rangle \rightarrow |m\rangle$ energy range actually help completing, on average, the required energy for the pumping of level $|i\rangle$, keeping the efficiency constant, at least for low enough temperatures, or keeping its decrease very slow for higher temperatures. Note, however, that in this frequency range, this higher efficiency comes at the cost of very low pumping power as we see below.

In fig. 6 we plot the power stored in the battery as a function of $\Delta\omega$. As expected, the power is maximized at resonance, $\omega_f = \omega_m$, for all temperatures. That is when the pumping rate, p , which depends on the inverse of $\Delta\omega^2$, reaches its maximum value for each set of fixed parameters, increasing the amount of energy injected in the system. Also note that, under the adiabatic elimination conditions, the stored power does not vary significantly with the temperature and it decays symmetrically as a function of $|\Delta\omega|$. The dependence of the input power with Ω is trivial ($P \propto \Omega^2$) and does not require a figure of its own.

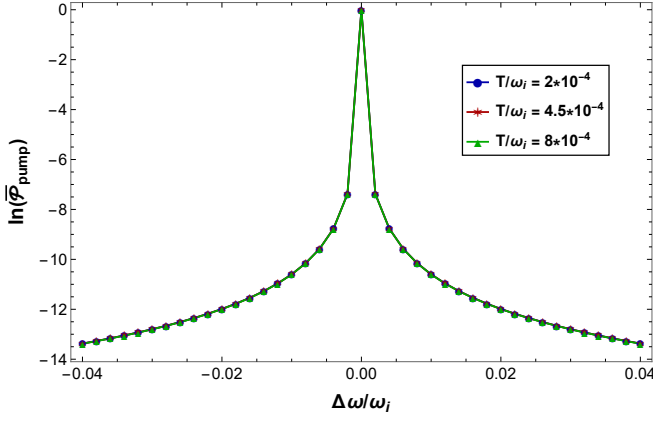


FIG. 6. We plot the logarithm of the normalized input power, $\bar{\mathcal{P}}_{\text{pump}} = \mathcal{P}_{\text{pump}}/\mathcal{P}_{\text{pump}}^{\text{max}}$, where $\mathcal{P}_{\text{pump}}$ is the input power and $\mathcal{P}_{\text{pump}}^{\text{max}}$ is the maximum input power obtained at $\Delta\omega = 0$ ($\omega_f = \omega_m$), as a function of $\Delta\omega/\omega_i$ for different temperatures. In both figures we use the same set of parameters as in figure 5.

B. Quantum heat engine

We start by analyzing the performance of the two-stroke machine in the short cycle limit ($\sum_j \gamma_j \tau \ll 1$) which was previously proven to be the most efficient one. In this scenario, the efficiency and the output power are given by $\eta_{SC} = \mathcal{E}_{SC}/E_{in}^{SC}$ and $\mathcal{P}_{SC} = \mathcal{E}_{SC}/\tau$, respectively, where \mathcal{E}_{SC} is given by (20) and E_{in}^{SC} is calculated similarly to what was done for the quantum battery in section II B

In fig. 7, we plot the efficiency as a function of $\Delta\omega$. Note that, except for very low temperatures, η_{SC} is maximized at resonance, $\omega_f = \omega_m$. Again, this happens because that is when the pumping rate, p , reaches its maximum value, injecting the most possible energy into the work fluid to be later extracted in the discharging stage. Contrary to the battery, however, the machine does not work at any temperature and for any detuning. Here, it is not enough to take the system out of thermal equilibrium by storing some energy in it. By design, the machine requires positive ergotropy after the recharging stage, which is achieved for $\rho_{ii} > \rho_{ee}$ and this condition cannot be matched if T is too high and/or p is too low. In fact, as the temperature of the natural reservoir increases, so does the thermal population of level $|e\rangle$. This requires more pumping power to invert the population in the $\{|e\rangle, |i\rangle\}$ subspace limiting the operation of the machine to detunings around the resonance. The higher the temperature, the closer to resonance one needs to pump. In fact, as we see in Fig. 8, there is a temperature threshold beyond which the machine does not work, no matter how strongly we pump. We comment more on this later in this section.

Thermal fluctuations also do affect the overall efficiency of the machine in the short cycle but in a much smaller scale than its range of operation, i.e. as long as

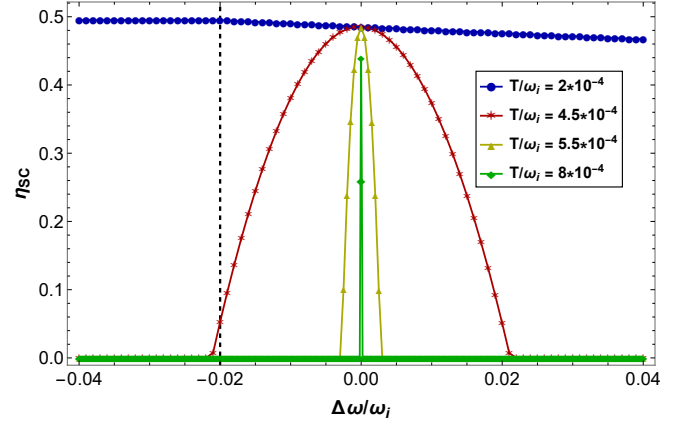


FIG. 7. We plot the efficiency of the machine as a function of $\Delta\omega/\omega_i$ in the short cycle (SC) limit for different temperatures. Parameters: $\Omega/\omega_i = 10^{-8}$, $\gamma_0^m/\omega_i = 10^{-4}$, $\gamma_0^i/\omega_i = \gamma_0^e/\omega_i = 10^{-7}$, $\omega_e/\omega_i = 0.01$ and $\omega_m/\omega_i = 1.02$.

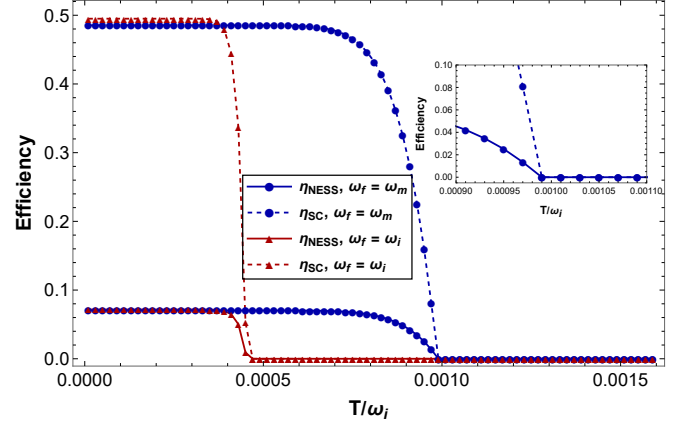


FIG. 8. Here we plot the efficiency in the asymptotic cycle, η_{NESS} and the efficiency in the short cycle, η_{SC} , for different values of the frequency of the external drive, ω_f , as a function of the temperature of the natural thermal reservoir. Parameters: $\Omega/\omega_i = 10^{-8}$, $\gamma_0^m/\omega_i = 10^{-4}$, $\gamma_0^i/\omega_i = \gamma_0^e/\omega_i = 10^{-7}$, $\omega_e/\omega_i = 0.01$, $\omega_m/\omega_i = 1.02$ and $\epsilon/\omega_i = 2 \times 10^{-4}$ (for the asymptotic cycle).

the machine works, its efficiency is close to the maximum for a given pumping frequency.

As we have seen in section II C, the efficiency of the short cycle is maximized when $\frac{\Gamma_i^+}{\gamma_i^-} \gg \frac{\gamma_e^+}{\gamma_e^-}$. If we consider a standard thermal reservoir, then one of the ways to achieve this limit is to operate coupled to a very low temperature ($T \ll 1$) and in resonance. In this limit, $\Gamma_i^+ \sim p\gamma_m^-$, $\gamma_e^+ \approx 0$ and the efficiency of the short cycle is approximated by

$$\eta_{SC} \approx \frac{\gamma_e^-}{\gamma_e^- + \gamma_i^-} \frac{\omega_i - \omega_e}{\omega_m} = \frac{\gamma_e^-}{\gamma_e^- + \gamma_i^-} \frac{\omega_i - \omega_e}{\omega_i} \frac{1}{1 + \frac{\delta\omega}{\omega_i}}, \quad (21)$$

where $\delta\omega = \omega_m - \omega_i$. This result approaches the efficiency of the Otto cycle operating in a three-level scheme,

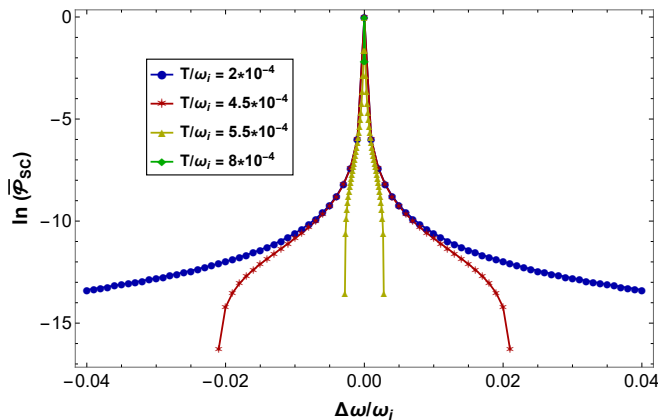


FIG. 9. We plot the logarithm of the normalized output power, $\bar{P}_{SC} = P_{SC}/P_{SC}^{max}$, where P_{SC} is the output power and P_{SC}^{max} is the maximum output power, as a function of $\Delta\omega/\omega_i$ for different temperatures. Here we use the same parameters as in fig. 7.

$\eta_{Otto} = \frac{\omega_i - \omega_e}{\omega_i}$, when $\gamma_e^- \gg \gamma_i^-$. η_{Otto} was shown to be the efficiency of this two-stroke machine operating under thermal reservoirs of temperatures T_H and T affecting respectively the $|g\rangle \rightarrow |i\rangle$ and the $|g\rangle \rightarrow |e\rangle$ transitions [77]. The extra factor $\frac{1}{1 + \frac{\delta\omega}{\omega_i}}$, that reduces this efficiency, comes from the energy wasted to generate the effective temperature T_H through optically pumping level $|m\rangle$. Note that, as long as $\delta\omega \ll \omega_i$, this correction amounts to a small linear decay of the efficiency proportional to $\frac{\delta\omega}{\omega_i}$. This factor, however, cannot be made as small as possible because there must be a minimum energy separation between levels $|i\rangle$ and $|m\rangle$ to make it possible to adiabatically eliminate the latter.

The other relevant figure of merit of the heat machine is its output power. In fig. 9 we see that this quantity reaches its maximum value when the external source drives the $|g\rangle \rightarrow |m\rangle$ transition resonantly, $\omega_f = \omega_m$, and decays symmetrically around it. We also note that around resonance, $\omega_f \sim \omega_m$, as long as the positive ergotropy condition is achieved, the output power does not depend significantly on the temperature of the natural reservoir. However, as previously analysed, the higher the temperature, the closer to resonance one needs to be for the machine to operate.

From the efficiency and power analysis, we can state that, as in the quantum battery, the machine works better in the regime of low temperature. It is worth noting that the short cycle gives the best performance but the output power per cycle, that is proportional to the stored ergotropy, is very small. That is the downside of maximizing the efficiency.

We can also analyse the performance of the machine operating in the limit of the asymptotic cycle, i.e. when the duration of the recharging stage, τ_r is set to allow the battery to store close to its maximum capacity. In this limit, the operational steady state, ρ_{OSS} , converges to ρ_{NESS} and the efficiency and the output power are

given by $\eta = -W_{ext}/E_{in}$ and $\mathcal{P} = -W_{ext}/\tau$, respectively, where W_{ext} is calculated via Eq. (3). In fig. 8 we plot the efficiency of both the short and long cycles as a function of the temperature for two pumping frequencies. Note that, for a given detuning, the temperature threshold is the same for both cycles. The largest threshold, on the other hand, is found at resonance ($\omega_f = \omega_m$) whereas, for fixed couplings to the external drive, larger detunings lower the temperature threshold, as expected.

The dependence of the output power with the duration of the cycle is the same as the one observed in previous works [43, 77]: the power is maximized for the short cycle and decays as the cycle duration increases. Considering that the output power is the ratio between the extracted work and the duration of the cycle τ , that means that the increase in the extraction of work grows slower than linearly with τ , the linear increase being the one obtained exactly in the short cycle.

IV. CONCLUSION

This work have encompassed two studies: first, we have studied the optical pumping of a quantum battery from the perspective of the efficiency, the input power and the total energy stored in the process. We have concentrated our analysis in a cascade three-level scheme where the upper energy level is adiabatically eliminated from the dynamics. In this particular scenario, we have found that there is no universal optimal set of parameters to charge the battery. The process is more efficient for short times, in a time scale comparable with the adiabatic elimination condition, dominated by the decay rate of the accessory higher energy level $|m\rangle$ ($t \sim 1/\gamma_m^-$). This is consistent with the idea that the stabilization of the population of the eliminated level marks the moment in time when most of the pumped energy is directly transferred to the optically pumped target level of the battery. This is the best achievable efficiency in the process but, in this time scale, the battery is still quite empty. The other meaningful time scale is the one to the fully charge the battery, connected to the decay time of the optically pumped level ($t \sim 1/\gamma_i^-$). At this time scale, the battery stores as much power as possible but the overall efficiency drops because some of the pumped energy is lost in the form of heat. We have also shown that, as long as the adiabatic elimination is still valid, i.e. as long as the temperature of the dissipative thermal reservoir is not too high, temperature does not affect significantly the charging process. Finally, the charging process is slightly more efficient when the pumping frequency matches that of the pumped transition ($\omega_f = \omega_i$) but at the cost of a much larger loss of the stored power. That justifies choosing the resonance condition ($\omega_f = \omega_m$) as the best charging protocol.

The second part of the work regards using the battery as the working fluid of a two-stroke thermal machine. Once again, best performance is achieved operating at

low temperature and in short cycles. The maximum efficiency approaches that of an equivalent machine running an Otto cycle and is obtained when the machine operates at very low temperatures and in short cycles. The correcting factor that reduces the Otto cycle efficiency comes from the energy wasted to create the effective high temperature through the optical pumping mechanism and can be made small as long as the adiabatically eliminated level is not much more energetic than the optically pumped one. The Otto cycle efficiency cannot be achieved, though, because for the adiabatic elimination to work, some energy separation is still required between the levels.

Still concerning the short cycle and similarly to the charging of the battery, highest efficiency is achieved when the pumping frequency matches the Bohr frequency of the optically pumped transition ($\omega_f = \omega_i$). However, differently from the first part of the work, the analysed two-stroke machine cannot operate at any combination of pump frequency and temperature. The higher the cold reservoir temperature, the closer to resonance ($\omega_f \sim \omega_m$) the machine needs to be. On the other hand, in resonance and as long as the machine is able to operate, its efficiency is not significantly affected by the temperature of the cold reservoir. The shutdown transition due to the temperature raise is quite sharp.

We also analysed the machine under the asymptotic cycle, where the battery is allowed to be fully charged in the recharging state. We have shown that it has the same shutdown temperature of the short cycle, i.e. the threshold temperature of the cold reservoir beyond which work extraction stops is the same regardless of the duration of the cycle. Efficiency and output power are both lower in this regime, however, as it has already been shown in previous works [43, 77].

Finally, it is worth mentioning that the models adopted here can be adapted to different quantum optical setups. Both the quantum battery and the heat engine can be implemented in both natural and artificial atoms, superconducting circuits and similar systems.

V. ACKNOWLEDGMENTS

M.F.S. acknowledges FAPERJ Project No. E-26/202.576/2019 and CNPq Projects No. 302872/2019-1 and INCT-IQ 465469/2014-0. T.F.F.S. acknowledges CAPES for financial support.

VI. APPENDIX

Here we show more details about the calculations of the results shown in the main text.

A. Quantum Battery

1. Adiabatic Elimination

The dynamics of the system is described by a master equation in the Lindblad form ($\hbar = 1$ and $k_B = 1$):

$$\dot{\rho}(t) = -i[H(t), \rho(t)] + \mathcal{L}[\rho(t)]. \quad (22)$$

The Hamiltonian reads $H(t) = H_0 + V(t)$, where H_0 is the free Hamiltonian of the system and $V(t)$ account for coupling with an external work source. For the quantum battery model, we have $V(t) = V_{in}(t)$, where $V_{in}(t)$ is given by

$$V_{in}(t) = \Omega (|g\rangle \langle m| e^{i\omega_f t} + |m\rangle \langle g| e^{-i\omega_f t}). \quad (23)$$

The non-unitary part of the dynamics, represented by $\mathcal{L}[\rho(t)]$, is given by

$$\mathcal{L}[\rho(t)] = \mathcal{L}_{\gamma_m}[\rho(t)] + \mathcal{L}_{\gamma_i}[\rho(t)], \quad (24)$$

where $\mathcal{L}_{\gamma_m}[\rho(t)]$ and $\mathcal{L}_{\gamma_i}[\rho(t)]$ are given by Eqs. (5) and (6), respectively.

In a rotating framework, defined by $\varrho(t) = e^{iH'_0 t} \rho e^{-iH'_0 t}$, where $H'_0 = H_0 + \Delta\omega |m\rangle \langle m|$ and $\Delta\omega = \omega_f - \omega_m$, Eq. 22 reads

$$\dot{\varrho}(t) = -i[\bar{V}, \varrho(t)] + \mathcal{L}[\varrho(t)], \quad (25)$$

where

$$\bar{V}_{in} = \Omega(|g\rangle \langle m| + |m\rangle \langle g|) - \Delta\omega |m\rangle \langle m|. \quad (26)$$

and $\mathcal{L}[\varrho(t)]$, is the same as in Eq. (??).

If $\gamma_m^- \gg \gamma_m^+, \gamma_i^\pm, \Omega$, we can adiabatically eliminate level $|m\rangle$ and its coherences ($\{\rho_{mi}, \rho_{im}\}$). In particular, we obtain

$$\varrho_{mm} \approx \frac{1}{\gamma_m^-} [p\gamma_m^- \varrho_{gg} + \gamma_m^+ \varrho_{ii}], \quad (27)$$

where $p = \frac{4\Omega^2}{\gamma_m^{-2} + 4\Delta\omega^2} \ll 1$, and

$$\varrho_{mg} - \varrho_{gm} \approx -\frac{4i\Omega}{\gamma_m^{-2} + 4\Delta\omega^2} \gamma_m^- (\varrho_{gg} - \varrho_{mm}). \quad (28)$$

for the time evolution of the variables related to level $|m\rangle$.

Substituting Eq. (27) in the equation of motion for level $|i\rangle$, we end up with

$$\dot{\varrho}_{ii}(t) = \Gamma_i^+ \varrho_{gg} - \gamma_i^- \varrho_{ii}, \quad (29)$$

where $\Gamma_i^+ = \gamma_i^+ + p\gamma_m^-$. For level $|g\rangle$ and the coherence between level $|g\rangle$ and $|i\rangle$, we obtain

$$\dot{\varrho}_{gi}(t) = \gamma_i^- \varrho_{ii} - \Gamma_i^+ \varrho_{gi}, \quad (30)$$

and

$$\dot{\varrho}_{gi}(t) = -ip\Delta\omega \varrho_{gi} - (\Gamma_i^+ + \gamma_i^-) \varrho_{gi}. \quad (31)$$

Using these equations we can, finally, write a master equation for the effective qutrit in the Lindblad form

$$\begin{aligned}\dot{\varrho}(t) = & -i[\bar{V}_{eff}, \varrho(t)] \\ & + \frac{\Gamma_i^+}{2}(2|i\rangle\langle g|\varrho(t)|g\rangle\langle i| - \{|g\rangle\langle g|, \varrho(t)\}) \\ & + \frac{\gamma_i^-}{2}(2|g\rangle\langle i|\varrho(t)|i\rangle\langle g| - \{|i\rangle\langle i|, \varrho(t)\})\end{aligned}\quad (32)$$

where $\bar{V}_{eff} = p\Delta\omega|g\rangle\langle g|$ and $\{A, B\} = AB + BA$. This equation are the same as the ones for a qubit in contact with a thermal reservoir at temperature $T_H = \frac{\hbar\omega_i}{k_B \ln(\frac{\gamma_i^-}{p\gamma_m^- + \gamma_i^+})}$.

2. Thermodynamics

The efficiency of the pumping process, η_{pump} , and its input power, \mathcal{P}_{pump} , are defined respectively by

$$\eta_{pump} = \frac{\Delta F}{E_{in}} \quad (33)$$

and

$$\mathcal{P}_{pump} = \frac{\Delta F}{\tau}, \quad (34)$$

where ΔF is the variation of the Helmholtz free energy during the process, from $t_0 = 0$ to $t = \tau$. and E_{in} is the energy injected into the system

$$E_{in} = \text{Max}\{W_{in}, W_{in} + Q_{\gamma_m}, W_{in} + Q_{\gamma_i}, W_{in} + Q\}. \quad (35)$$

Here W_{in} is the work done on the system, given by

$$\begin{aligned}W_{in} &= \int_0^\tau dt \text{Tr}\{\rho(t)\dot{V}_{in}(t)\} \\ &= \int_{t_0}^{t_f} dt \text{Tr}\{\rho^j[i\Omega\omega_f(|g\rangle\langle m|e^{i\omega_f t} - |m\rangle\langle g|e^{-i\omega_f t})]\} \\ &= \int_{t_0}^{t_f} dt i\Omega\omega_f[\rho_{mg}(t)e^{i\omega_f t} - \rho_{gm}(t)e^{-i\omega_f t}] \\ &= i\Omega\omega_f \int_0^\tau dt [\varrho_{mg}(t) - \varrho_{gm}(t)],\end{aligned}\quad (36)$$

where $\varrho = e^{iH_0 t} \rho e^{-iH_0 t}$. Q_{γ_m} is the heat exchange associated with the transitions between levels $|i\rangle$ and $|m\rangle$,

$$\begin{aligned}Q_{\gamma_m} &= \int_0^\tau dt \text{Tr}[\mathcal{L}_{\gamma_m}[\rho(t)]H(t)] \\ &= -\Omega \frac{\gamma_m^-}{2} \int_0^\tau dt [\varrho_{mg}(t) + \varrho_{gm}(t)] \\ &\quad + (\omega_m - \omega_i) \int_0^\tau dt [\gamma_m^+ \varrho_{ii}(t) - \gamma_m^- \varrho_{mm}(t)],\end{aligned}\quad (37)$$

Q_{γ_i} with the transitions between levels $|g\rangle$ and $|i\rangle$,

$$\begin{aligned}Q_{\gamma_i} &= \int_0^\tau dt \text{Tr}[\mathcal{L}_{\gamma_i}[\rho(t)]H(t)] \\ &= -\Omega \frac{\gamma_i^+}{2} \int_0^\tau dt [\varrho_{mg}(t) + \varrho_{gm}(t)] \\ &\quad + \omega_i \int_0^\tau dt [\gamma_i^+ \varrho_{gg}(t) - \gamma_i^- \varrho_{ii}(t)]\end{aligned}\quad (38)$$

and $Q = Q_{\gamma_m} + Q_{\gamma_i}$ is the total heat exchange in the system.

In the adiabatic elimination regime, substituting Eq. (28) in Eq. (36), we obtain

$$W_{in} = p\gamma_m^- \omega_f \int_0^\tau dt (\varrho_{gg}(t) - \varrho_{mm}(t)). \quad (39)$$

In this limit, $\varrho_{gg} \gg \varrho_{mm}$, and

$$W_{in} \approx p\gamma_m^- \omega_f \int_0^\tau dt \varrho_{gg}(t). \quad (40)$$

We can make similar approximations for the calculation of the heat exchange. The sum of the coherences is approximately given by

$$\varrho_{mg}(t) + \varrho_{gm}(t) \approx \frac{8\Omega}{\gamma_m^{-2} + 4\Delta\omega^2} \Delta\omega(\varrho_{gg}(t) - \varrho_{mm}(t)), \quad (41)$$

and substituting this expression and Eq. (27) in Eqs. (37) and (38), we obtain

$$\begin{aligned}Q_{\gamma_m} &\approx -p\gamma_m^- \Delta\omega \int_0^\tau dt \varrho_{gg}(t) \\ &\quad - (\omega_m - \omega_i) p\gamma_m^- \int_0^\tau dt \varrho_{gg}(t) \\ &= p\gamma_m^- (\omega_i - \omega_f) \int_0^\tau dt \varrho_{gg}(t)\end{aligned}\quad (42)$$

and

$$\begin{aligned}Q_{\gamma_i} &= -p\gamma_i^+ \Delta\omega \int_0^\tau dt \varrho_{gg}(t) \\ &\quad + \omega_i \int_0^\tau dt (\gamma_i^+ \varrho_{gg}(t) - \gamma_i^- \varrho_{ii}(t)).\end{aligned}\quad (43)$$

Once again, we consider that $\varrho_{gg} \gg \varrho_{mm}$.

For $T = 0$, $\gamma_k^- = \gamma_0^k$ and $\gamma_k^+ = 0$. This condition simplifies the calculation for the variation of the Helmholtz free energy

$$\Delta F = \omega_i p_i(t), \quad (44)$$

and the equations of motion of the system. In the examples given in the main text we assume a recharging time τ large enough for the system to reach ρ_{NESS} . Under this condition, we obtain, for the Helmholtz free energy and the energy injected into the system,

$$\Delta F = \omega_i p_i^{NESS} = \omega_i \frac{p\gamma_0^m}{\gamma_0^i + p\gamma_0^m}, \quad (45)$$

$$E_{in} \approx p\gamma_0^m \omega_i \frac{\gamma_0^i \tau}{\gamma_0^i + p\gamma_0^m}, \quad (46)$$

for $\omega_f < \omega_i$, and

$$E_{in} \approx p\gamma_0^m \omega_f \frac{\gamma_0^i \tau}{\gamma_0^i + p\gamma_0^m}, \quad (47)$$

for $\omega_f \geq \omega_i$. Calculating the efficiency in this scenario we obtain,

$$\eta_{Max} = \frac{\Delta F}{E_{in}} \approx \frac{1}{\gamma_0^i \tau} \quad (48)$$

for $\omega_f < \omega_i$, and

$$\eta_{pump} = \frac{\Delta F}{E_{in}} \approx \left(1 - \frac{\Delta f_i}{\omega_i}\right) \eta_{Max}, \quad (49)$$

for $\omega_f \geq \omega_i$. The maximum efficiency is obtained in $T = 0$, as it can be seen in the examples given in the main text. The efficiency decreases with the increase of the temperature of the natural reservoir.

B. Quantum heat engine

1. Adiabatic Elimination

The calculations for the adiabatic elimination of the level $|m\rangle$ for the two stroke quantum heat engine are similar to those of the quantum battery. The dynamics of the system is also described by a master equation in the Lindblad form, given by Eq. (22). The quantum heat engine includes a fourth level, $|e\rangle$, so the non-unitary part of the dynamics has an extra term and given by

$$\mathcal{L}[\rho(t)] = \mathcal{L}_{\gamma_m}[\rho(t)] + \mathcal{L}_{\gamma_i}[\rho(t)] + \mathcal{L}_{\gamma_e}[\rho(t)], \quad (50)$$

where $\mathcal{L}_{\gamma_m}[\rho(t)]$ and $\mathcal{L}_{\gamma_i}[\rho(t)]$ are given by Eqs. (5) and (6), respectively, and $\mathcal{L}_{\gamma_e}[\rho(t)]$ is given by (15).

For the unitary part of the dynamics we have that in the discharging stage $V(t)$ has an extra term, V_{ext} , that extracts the energy stored in the system in the form of work and is given by

$$V_{ext}(t) = \epsilon \left(|e\rangle \langle i| e^{i(\omega_i - \omega_e)t} + |i\rangle \langle e| e^{-i(\omega_i - \omega_e)t} \right). \quad (51)$$

In the recharging stage we have that $V(t) = V_{in}(t)$, as in the quantum battery, given by Eq. (23).

In the same rotating framework used before, the master equation for the engine becomes

$$\dot{\rho}(t) = -i[\bar{V}, \rho(t)] + \mathcal{L}(\rho(t)), \quad (52)$$

where in the discharging stage we have

$$\begin{aligned} \bar{V} &= \bar{V}_{ext} + \bar{V}_{in} \\ &= \epsilon(|e\rangle \langle i| + |i\rangle \langle e|) \\ &\quad + \Omega(|g\rangle \langle m| + |m\rangle \langle g|) - \Delta\omega |m\rangle \langle m|. \end{aligned} \quad (53)$$

and in the recharging stage we have

$$\bar{V} = \Omega(|g\rangle \langle m| + |m\rangle \langle g|) - \Delta\omega |m\rangle \langle m|. \quad (54)$$

Once again, considering that $\gamma_m^- \gg \gamma_m^+, \gamma_{e(i)}^\pm, \Omega$, we obtain approximate solutions for the time evolution of the population and coherences of level $|m\rangle$. Here, however, we must also assume that $\gamma_{e(i)}^- \gg \gamma_m^+$. By doing so, we obtain the following master equation for the effective qutrit of levels $|g\rangle$, $|e\rangle$ and $|i\rangle$:

$$\begin{aligned} \dot{\rho}(t) &= -i[\bar{V}_{eff}, \rho(t)] \\ &\quad + \frac{\Gamma_i^+}{2} (2|i\rangle \langle g| \rho(t) |g\rangle \langle i| - \{|g\rangle \langle g|, \rho(t)\}) \\ &\quad + \frac{\gamma_i^-}{2} (2|g\rangle \langle i| \rho(t) |i\rangle \langle g| - \{|i\rangle \langle i|, \rho(t)\}) \\ &\quad + \frac{\gamma_e^+}{2} (2|e\rangle \langle g| \rho(t) |g\rangle \langle e| - \{|g\rangle \langle g|, \rho(t)\}) \\ &\quad + \frac{\gamma_e^-}{2} (2|g\rangle \langle e| \rho(t) |e\rangle \langle g| - \{|e\rangle \langle e|, \rho(t)\}), \end{aligned} \quad (55)$$

where $\bar{V}_{eff} = p\Delta\omega |g\rangle \langle g|$, $\Gamma_i^+ = \gamma_i^+ + p\gamma_m^-$ and $\{A, B\} = AB + BA$.

C. Calculations for the short cycle limit

In this section, we use the conditions of the adiabatic elimination of $|m\rangle$ to calculate the thermodynamic quantities of interest for the machine operating in the limit of short cycles ($\sum_j \gamma_j^\pm \tau \ll 1$, where τ is the duration of the cycle).

For the short cycle, the operational steady state is obtained solving the equation $\rho_{OSS} = \tilde{\rho}_{OSS} + \tau \mathcal{L}(\tilde{\rho}_{OSS})$, where $\tilde{\rho}_{OSS} = U \rho U^{-1}$, $U = -i(|i\rangle \langle e| + |e\rangle \langle i|) + |g\rangle \langle g| + |m\rangle \langle m|$ and the coupling with the thermal reservoir, $\mathcal{L}(\tilde{\rho}_{OSS})$, is given by equation (24).

In the rotating reference frame, the equation of motion for the populations and for the coherences between levels $|g\rangle$ and $|m\rangle$ are given by

$$i\Omega(r_{mg} - r_{gm}) = \gamma_e^- r_i + \gamma_i^- r_e - (\gamma_e^+ + \gamma_i^+) r_g, \quad (56)$$

$$-i\Omega(r_{mg} - r_{gm}) = \gamma_m^+ r_e - \gamma_m^- r_m, \quad (57)$$

$$r_i - r_e = [\gamma_i^+ r_g + \gamma_m^- r_m - (\gamma_m^+ + \gamma_i^-) r_e] \tau, \quad (58)$$

$$r_e - r_i = [\gamma_e^+ r_g - \gamma_e^- r_i] \tau, \quad (59)$$

$$2i\Omega(r_g - r_m) = (\gamma_e^+ + \gamma_i^+ + \gamma_m^- + 2i\Delta\omega) r_{gm}, \quad (60)$$

where $r_{jk} = \langle j | \rho | k \rangle$. Using Eq. (60) and its complex conjugate, we obtain

$$r_{mg} - r_{gm} = -\frac{4i\Omega\alpha}{\alpha^2 + 4\Delta\omega^2} (r_g - r_m). \quad (61)$$

Under the adiabatic elimination conditions, this expression becomes

$$r_{mg} - r_{gm} = -\frac{4i\Omega}{\gamma_m^{-2} + 4\Delta\omega^2} \gamma_m^- (r_g - r_m). \quad (62)$$

Note that, since $r_m \ll r_g$, we can simplify the expression above to

$$r_{mg} - r_{gm} \approx -\frac{4i\Omega}{\gamma_m^{-2} + 4\Delta\omega^2} \gamma_m^- r_g. \quad (63)$$

Substituting Eq. (63) in Eq. (56), we obtain

$$r_g = \frac{\gamma_e^- r_i + \gamma_i^- r_e}{\Gamma_i^+ + \gamma_e^+}, \quad (64)$$

where, $\Gamma_i^+ = \gamma_i^+ + p\gamma_m^-$ and $p = \frac{4\Omega^2}{\gamma_m^{-2} + 4\Delta\omega^2} \ll 1$.

Substituting Eq. (63) in Eq. (57), we obtain

$$\gamma_m^- r_m = \gamma_m^+ r_e + p\gamma_m^- r_g. \quad (65)$$

From the Eq. (59), we obtain

$$r_e = \frac{r_i [1 - (\gamma_e^+ + \gamma_e^-)\tau] + \gamma_e^+ \tau}{1 + \gamma_e^+ \tau}. \quad (66)$$

Substituting Eqs. (64) and (66) in Eq. (58) and doing some algebraic manipulation we obtain

$$r_i = \frac{\Gamma_i^+ + \gamma_e^+ - \gamma_e^+ \gamma_i^- \tau}{2(\Gamma_i^+ + \gamma_e^+) + \gamma_i^- + \gamma_e^- - [\gamma_e^- (\Gamma_i^+ + \gamma_i^-) + \gamma_e^+ \gamma_i^-]} \tau. \quad (67)$$

Using the relations between r_e and r_i and keeping terms up to first order in τ , the ergotropy, given by $\mathcal{E}^V = (\omega_i - \omega_e)(r_i - r_e)$, becomes

$$\mathcal{E}^{SC} = \frac{\omega_i - \omega_e}{2(\Gamma_i^+ + \gamma_e^+) + \gamma_i^- + \gamma_e^-} (\Gamma_i^+ \gamma_e^- - \gamma_i^- \gamma_e^+) \tau. \quad (68)$$

Note that, for the ergotropy to be positive it is necessary that $\frac{\Gamma_i^+}{\gamma_i^-} > \frac{\gamma_e^+}{\gamma_e^-}$. It means that the temperature of the effective reservoir, T_i , that appears due to the adiabatic elimination procedure, has to be larger than the temperature of the thermal reservoir, T . For the output power, defined as $\mathcal{P}^{SC} = \mathcal{E}^{SC}/\tau$, we have

$$\mathcal{P}^{SC} = (\omega_i - \omega_e) \frac{\Gamma_i^+ \gamma_e^- - \gamma_i^- \gamma_e^+}{2(\Gamma_i^+ + \gamma_e^+) + \gamma_i^- + \gamma_e^-}. \quad (69)$$

The efficiency of the short cycle is defined by

$$\eta^{SC} = \frac{\mathcal{E}^{SC}}{E_{in}^{SC}}, \quad (70)$$

where E_{in}^{SC} is the energy injected into the system in the cycle, given by

$$E_{in}^{SC} = \text{Max}\{W_{in}^{SC}, W_{in}^{SC} + Q_{in}^{SC}, W_{in}^{SC} + Q_{\gamma_m}^{SC}, W_{in}^{SC} + Q_{\gamma_i}^{SC}, W_{in}^{SC} + Q_{\gamma_e}^{SC}\} \quad (71)$$

where W_{in}^{SC} is the work done on the system due to its coupling to the external work source represented by $V_{in}(t)$,

$$\begin{aligned} W_{in}^{SC} &= \text{Tr}\{\rho(\tau) \dot{V}_{in}(\tau)\} \tau \\ &= \text{Tr}\{\rho(\tau) [i\omega_f \Omega (|g\rangle \langle m| e^{i\omega_f \tau} - |m\rangle \langle g| e^{-i\omega_f \tau})]\} \tau \\ &= i\omega_f \Omega (\rho_{mg} e^{i\omega_f \tau} - \rho_{gm} e^{-i\omega_f \tau}) \tau \\ &= i\omega_f \Omega (r_{mg} - r_{gm}) \tau. \end{aligned} \quad (72)$$

Substituting Eq. (63) in Eq. (72), we obtain

$$\begin{aligned} W_{in}^{SC} &\approx p\omega_f \gamma_m^- r_g \tau \\ &= p\omega_f \gamma_m^- \frac{\gamma_e^- + \gamma_i^-}{\kappa} \tau, \end{aligned} \quad (73)$$

where $\kappa = 2(\Gamma_i^+ + \gamma_e^+) + \gamma_i^- + \gamma_e^-$. The total heat exchange between the system and the reservoir, Q_{SC} is given by

$$Q_{SC} = Q_{\gamma_e}^{SC} + Q_{\gamma_i}^{SC} + Q_{\gamma_m}^{SC}, \quad (74)$$

where, Q_e is the heat exchange associated with the transitions between levels $|e\rangle$ and $|g\rangle$

$$\begin{aligned} Q_{\gamma_e}^{SC} &= \text{Tr}\{\mathcal{L}_{\gamma_e}[\tilde{\rho}][H_0 + V_{in}(\tau)]\} \tau \\ &= \omega_e \tau (\gamma_e^+ r_g - \gamma_e^- r_i) - \gamma_e^+ \frac{\omega}{2} \tau (r_{mg} + r_{gm}) \\ &= \omega_e \frac{\gamma_e^+ \gamma_i^- - \Gamma_i^+ \gamma_e^-}{\kappa} \tau - p\gamma_e^+ \Delta\omega \frac{\gamma_i^- + \gamma_e^-}{\kappa} \tau, \end{aligned} \quad (75)$$

where

$$\begin{aligned} r_{mg} + r_{gm} &= \frac{8\Omega\Delta\omega}{\gamma_m^{-2} + 4\Delta\omega^2} (r_g - r_m) \\ &\approx \frac{8\Omega\Delta\omega}{\gamma_m^{-2} + 4\Delta\omega^2} r_g, \end{aligned} \quad (76)$$

Q_i is the heat exchange associated with the transitions between levels $|i\rangle$ and $|g\rangle$

$$\begin{aligned} Q_{\gamma_i}^{SC} &= \text{Tr}\{\mathcal{L}_{\gamma_i}[\tilde{\rho}][H_0 + V_{in}(\tau)]\} \tau \\ &= \omega_i \tau (\gamma_i^+ r_g - \gamma_i^- r_e) - \gamma_i^+ \frac{\omega}{2} \tau (r_{mg} + r_{gm}) \\ &= \omega_i \frac{\gamma_i^+ \gamma_e^- - \gamma_i^- (\gamma_e^+ + p\gamma_m^-)}{\kappa} \tau \\ &\quad - p\gamma_i^+ \Delta\omega \frac{\gamma_i^- + \gamma_e^-}{\kappa} \tau, \end{aligned} \quad (77)$$

and Q_m is the heat exchange associated with the transitions between levels $|m\rangle$ and $|i\rangle$

$$\begin{aligned} Q_{\gamma_m}^{SC} &= \text{Tr}\{\mathcal{L}_{\gamma_m}[\tilde{\rho}][H_0 + V_{in}(\tau)]\} \tau \\ &= (\omega_i - \omega_m) \tau (\gamma_m^- r_m - \gamma_m^+ r_e) - \gamma_m^- \frac{\Omega}{2} \tau (r_{mg} + r_{gm}) \\ &= (\omega_i - \omega_m) \tau i\Omega (r_{mg} - r_{gm}) - \gamma_m^- \frac{\Omega}{2} \tau (r_{mg} + r_{gm}) \\ &= (\omega_i - \omega_m) p\gamma_m^- \frac{\gamma_i^- + \gamma_e^-}{\kappa} \tau - p\gamma_m^- \Delta\omega \frac{\gamma_i^- + \gamma_e^-}{\kappa} \tau \\ &= (\omega_i - \omega_f) p\gamma_m^- \frac{\gamma_i^- + \gamma_e^-}{\kappa} \tau. \end{aligned} \quad (78)$$

In the regime of very low temperature, we have that for $\omega_f \geq \omega_i$

$$E_{in}^{SC} = W_{in}^{SC}, \quad (79)$$

and the efficiency is given by

$$\eta_{SC} = \left(\frac{\omega_i - \omega_e}{\omega_f} \right) \frac{\Gamma_i^+ \gamma_e^- - \gamma_i^- \gamma_e^+}{p \gamma_m^- (\gamma_i^- + \gamma_e^-)}. \quad (80)$$

We also have that $p \gamma_m^- \gg \gamma_{e(i)}^+$, $\gamma_j^- \approx \gamma_0$, and

$$\begin{aligned} \eta_{SC} &\approx \left(\frac{\omega_i - \omega_e}{\omega_f} \right) \frac{\gamma_0^e}{\gamma_0^e + \gamma_0^i} \\ &\approx \left(1 - \frac{\omega_e}{\omega_i} \right) \frac{\gamma_0^e}{\gamma_0^e + \gamma_0^i} \left(1 - \frac{\Delta_{fi}}{\omega_i} \right), \end{aligned} \quad (81)$$

where $\Delta_{fi} = \omega_f - \omega_i$.

For $\omega_f < \omega_i$, we have

$$E_{in}^{SC} = W_{in}^{SC} + Q_m^{SC}, \quad (82)$$

so the efficiency is given by

$$\eta_{SC} = \left(\frac{\omega_i - \omega_e}{\omega_i} \right) \frac{\Gamma_i^+ \gamma_e^- - \gamma_i^- \gamma_e^+}{p \gamma_m^- (\gamma_i^- + \gamma_e^-)}. \quad (83)$$

For temperatures low enough,

$$\eta_{SC} \approx \left(\frac{\omega_i - \omega_e}{\omega_i} \right) \frac{\gamma_0^e}{\gamma_0^e + \gamma_0^i}. \quad (84)$$

-
- [1] H. E. D. Scovil and E. O. Schulz-DuBois, Three-Level Masers as Heat Engines, *Phys. Rev. Lett.* **2**, 262 (1959).
 - [2] H. T. Quan, Yu-xi Liu, C. P. Sun, and F. Nori, Quantum thermodynamic cycles and quantum heat engines, *Phys. Rev. E* **76**, 031105 (2007).
 - [3] H. T. Quan, P. Zhang, and C. P. Sun, Quantum-classical transition of photon-Carnot engine induced by quantum decoherence, *Phys. Rev. E* **73**, 036122 (2006).
 - [4] H. T. Quan, P. Zhang, and C. P. Sun, Quantum heat engine with multilevel quantum systems, *Phys. Rev. E* **72**, 056110 (2005).
 - [5] C. M. Bender, D. C. Brody, and B. K. Meister, Quantum mechanical Carnot engine, *J. Phys. A* **33**, 4427 (2000).
 - [6] J. Arnaud, L. Chusseau, and F. Philippe, Carnot cycle for an oscillator, *Eur. J. Phys.* **23**, 489 (2002).
 - [7] F. Tonner and G. Mahler, Autonomous quantum thermodynamic machines, *Phys. Rev. E* **72**, 066118 (2005).
 - [8] Y. Rezek and R. Kosloff, Irreversible performance of a quantum harmonic heat engine, *New J. Phys.* **8**, 83 (2006).
 - [9] T. Feldmann and R. Kosloff, Quantum four-stroke heat engine: Thermodynamic observables in a model with intrinsic friction, *Phys. Rev. E* **68**, 016101 (2003).
 - [10] G. Thomas and R. S. Johal, Coupled quantum Otto cycle, *Phys. Rev. E* **83**, 031135 (2011).
 - [11] J. P. S. Peterson, T. B. Batalhão, M. Herrera, A. M. Souza, R. S. Sarthour, I. S. Oliveira, and R. M. Serra, Experimental characterization of a spin quantum heat engine, *Phys. Rev. Lett.* **123**, 240601 (2019).
 - [12] P. Skrzypczyk, A. J. Short, and S. Popescu, Work extraction and thermodynamics for individual quantum systems, *Nat. Commun.* **5**, 4185 (2014).
 - [13] R. Uzdin, A. Levy, and R. Kosloff, Equivalence of Quantum Heat Machines, and Quantum-Thermodynamic Signatures, *Phys. Rev. X* **5**, 031044 (2015).
 - [14] J. Klaers, S. Faelt, A. Imamoglu, and E. Togan, Squeezed Thermal Reservoirs as a Resource for a Nanomechanical Engine beyond the Carnot Limit, *Phys. Rev. X* **7**, 031044 (2017).
 - [15] N. Y. Halpern, C. D. White, S. Gopalakrishnan and G. Refael, Quantum engine based on many-body localization, *Phys. Rev. B* **99**, 024203 (2019).
 - [16] Giovanni Barontini and Mauro Paternostro, Ultra-cold single-atom quantum heat engines, *New J. Phys.* **21**, 063019 (2019).
 - [17] V. Shaghagh, G. Massimo Palma, and G. Benenti, Extracting work from random collisions: A model of a quantum heat engine, *Phys. Rev. E* **105**, 034101 (2022).
 - [18] K. Ptaszyński, Non-Markovian thermal operations boosting the performance of quantum heat engines, *Phys. Rev. E* **106**, 014114 (2022).
 - [19] R. Alicki, The quantum open system as a model of the heat engine, *J. Phys. A* **12**, L103 (1979).
 - [20] R. Kosloff, A quantum mechanical open system as a model of a heat engine, *J. Chem. Phys.* **80**, 1625 (1984).
 - [21] J. Roßnagel, S. T. Dawkins, K. N. Tolazzi, O. Abah, E. Lutz, F. Schmidt-Kaler, and K. Singer, A single-atom heat engine, *Science* **352**, 325 (2016).
 - [22] E. Geva and R. Kosloff, The quantum heat engine and heat pump: An irreversible thermodynamic analysis of the three-level amplifier, *J. Chem. Phys.* **104**, 7681 (1996).
 - [23] E. Geva and R. Kosloff, Three-level quantum amplifier as a heat engine: A study in finite-time thermodynamics, *Phys. Rev. E* **49**, 3903 (1994).
 - [24] V. Singh, Optimal operation of a three-level quantum heat engine and universal nature of efficiency, *Phys. Rev. Research* **2**, 043187 (2020).
 - [25] W. Niedenzu, M. Huber, and E. Boukobza, Concepts of work in autonomous quantum heat engines, *Quantum* **3**, 195 (2019).
 - [26] S. Bhattacharjee, U. Bhattacharya, W. Niedenzu, V.

- Mukherjee, and A. Dutta, Quantum magnetometry using two-stroke thermal machines, *New J. Phys.* **22**, 013024 (2020).
- [27] P. Menczel, C. Flindt, and K. Brandner, Thermodynamics of cyclic quantum amplifiers, *Phys. Rev. A* **101**, 052106 (2020).
- [28] A. Ghosh, D. Gelbwaser-Klimovsky, W. Niedenzu, A.I. Lvovsky, I. Mazets, M.O. Scully, and G. Kurizki, Two-level masers as heat-to-work converters. *Proc. Nat. Acad. Sci.* **115**, 9941 (2018).
- [29] A. Levy, L. Diósi, and R. Kosloff, Quantum flywheel, *Phys. Rev. A* **93**, 052119 (2016).
- [30] Md. Qutubuddin and K. E. Dorfman, Incoherent control of optical signals: Quantum-heat-engine approach, *Phys. Rev. Research* **3**, 023029 (2021).
- [31] Y. Zou, Y. Jiang, Y. Mei, X. Guo, and S. Du, Quantum Heat Engine Using Electromagnetically Induced Transparency, *Phys. Rev. Lett.* **119**, 050602 (2017).
- [32] V. Singh, Optimal operation of a three-level quantum heat engine and universal nature of efficiency, *Phys. Rev. Research* **2**, 043187 (2020).
- [33] Campaioli F., Pollock F.A., Vinjanampathy S. (2018) Quantum Batteries. In: Binder F., Correa L., Gogolin C., Anders J., Adesso G. (eds) *Thermodynamics in the Quantum Regime. Fundamental Theories of Physics*, vol **195**. Springer, Cham. https://doi.org/10.1007/978-3-319-99046-0_8
- [34] R. Alicki and M. Fannes, Entanglement boost for extractable work from ensembles of quantum batteries, *Phys. Rev. E* **87**, 042123, (2013).
- [35] F. C. Binder, S. Vinjanampathy, K. Modi & J. Goold, Quantacell: powerful charging of quantum batteries, *New Journal of Physics* **17**, 075015 (2015).
- [36] F. Campaioli, F. A. Pollock, F. C. Binder, L. Celeri, J. Goold, S. Vinjanampathy & K. Modi, Enhancing the Charging Power of Quantum Batteries, *Phys. Rev. Lett.* **118**, 150601 (2017).
- [37] D. Ferraro, M. Campisi, G. M. Andolina, V. Pellegrini & M. Polini, High-Power Collective Charging of a Solid-State Quantum Battery, *Phys. Rev. Lett.* **120**, 117702 (2018).
- [38] T. P. Le, J. Levinsen, K. Modi, M. M. Parish, and F. A. Pollock, Spin-chain model of a many-body quantum battery, *Phys. Rev. A* **97**, 022106 (2018).
- [39] G. M. Andolina, M. Keck, A. Mari, M. Campisi, V. Giovannetti and M. Polini, Extractable Work, the Role of Correlations, and Asymptotic Freedom in Quantum Batteries, *Phys. Rev. Lett.* **122**, 047702 (2019).
- [40] YY. Zhang, TR. Lang, L. Fu and X. Wang, Powerful harmonic charging in a quantum battery, *Phys. Rev. E* **99**, 052106.
- [41] A. Crescente, M. Carrega, M. Sassetti and D. Ferraro, Charging and energy fluctuations of a driven quantum battery, *New J. Phys.* **22** 063057 (2020).
- [42] D. Farina, G. M. Andolina, A. Mari, M. Polini and Vittorio Giovannetti, Charger-mediated energy transfer for quantum batteries: An open-system approach, *Phys. Rev. B* **99**, 035421 (2019).
- [43] F. Tacchino, T. F. F. Santos, D. Gerace, M. Campisi, and M. F. Santos, Charging a quantum battery via nonequilibrium heat current, *Phys. Rev. E* **102**, 062133 (2020).
- [44] F. Barra, Dissipative Charging of a Quantum Battery, *Phys. Rev. Lett.* **122**, 210601 (2019).
- [45] F. Primordial and K. Mølmer, Aging of a quantum battery, *Phys. Rev. A* **100**, 043833, (2019).
- [46] M. Carrega, A. Crescente, D. Ferraro and M. Sassetti, Dissipative dynamics of an open quantum battery, *New J. Phys.* **22** 083085 (2020).
- [47] A.C. Santos, B. Çakmak, S. Campbell and N.T. Zinner, Stable adiabatic quantum batteries, *Phys. Rev. E* **100**, 032107 (2019).
- [48] F. Caravelli, B. Yan, L.P. García-Pintos and A. Hama, Energy storage and coherence in closed and open quantum batteries, *Quantum* **5**, 505 (2021).
- [49] K. Xu, H. J. Zhu, G. F. Zhang, W. M. Liu, Enhancing the performance of an open quantum battery via environment engineering, *Phys. Rev. E* **104**, 064143 (2021).
- [50] Si-Yuan Bai and Jun-Hong An, Floquet engineering to reactivate a dissipative quantum battery, *Phys. Rev. A* **102**, 060201(R) (2020).
- [51] S. Zakavati, F. T. Tabesh, and S. Salimi, Bounds on charging power of open quantum batteries, *Phys. Rev. E* **104**, 054117 (2021).
- [52] Javier Carrasco, Jerónimo R. Maze, Carla Hermann-Avigliano, and Felipe Barra, Collective enhancement in dissipative quantum batteries, *Phys. Rev. E* **105**, 064119 (2022).
- [53] K. V. Hovhannisyan, M. Perarnau-Llobet, M. s Huber, and A. Acín, Entanglement Generation is Not Necessary for Optimal Work Extraction, *Phys. Rev. Lett.* **111**, 240401 (2013).
- [54] G. M. Andolina, D. Farina, A. a Mari, V. Pellegrini, V. Giovannetti, and M. o Polini, Charger-mediated energy transfer in exactly solvable models for quantum batteries, *Phys. Rev. B* **98**, 205423 (2018).
- [55] F. Caravelli, G. Coulter-De Wit, L. P. García-Pintos, and A. Hama, Random quantum batteries, *Phys. Rev. Research* **2**, 023095 (2020).
- [56] Sergi Julià-Farré, Tymoteusz Salamon, Arnau Riera, Manabendra N. Bera, and Maciej Lewenstein, Bounds on the capacity and power of quantum batteries, *Phys. Rev. Research* **2**, 023113 (2020).
- [57] S. Mondal and S. Bhattacharjee, Periodically driven many-body quantum battery, *Phys. Rev. E* **105**, 044125 (2022).
- [58] JY. Gyhm, D. Šafránek, and D. Rosa, Quantum Charging Advantage Cannot Be Extensive without Global Operations, *Phys. Rev. Lett.* **128**, 140501 (2022).
- [59] S. Ghosh and A. Sen, Dimensional enhancements in a quantum battery with imperfections, *Phys. Rev. A* **105**, 022628(2022).
- [60] JX. Liu, HL. Shi, YH. Shi, XH Wang, and WL. Yang, Entanglement and work extraction in the central-spin quantum battery, *Phys. Rev. B* **104**, 245418 (2021).
- [61] F. Mayo and A. J. Roncaglia, Collective effects and quantum coherence in dissipative charging of quantum batteries, *Phys. Rev. A* **105**, 062203 (2022).
- [62] K. V. Hovhannisyan, F. Barra, and A. Imparato, Charging assisted by thermalization, *Phys. Rev. Research* **2**, 033413 (2020).
- [63] F. Barra, K. V Hovhannisyan and A. Imparato, Quantum batteries at the verge of a phase transition, *New J. Phys.* **24** 015003 (2022).
- [64] S. Ghosh, T. Chanda, S. Mal, and A. Sen, Fast charging of a quantum battery assisted by noise, *Phys. Rev. A* **104**, 032207 (2021).
- [65] Stig Stenholm, *Foundations of Laser Spectroscopy* (Dover Publications, 2012).

- [66] Pierre Meystre, *Atom Optics* (Springer, 2001).
- [67] H. P. Breuer and F. Petruccione, *The theory of open quantum systems* (Oxford University Press, 2002).
- [68] F. Binder, S. Vinjanampathy, K. Modi, J. Goold, Quantum thermodynamics of general quantum processes, *Phys. Rev. E* **91**, 032119 (2015).
- [69] K. Funo and H. T. Quan, Path Integral Approach to Quantum Thermodynamics, *Phys. Rev. Lett.* **121**, 040602 (2018).
- [70] B. de Lima Bernardo, Unraveling the role of coherence in the first law of quantum thermodynamics, *Phys. Rev. E* **102**, 062152 (2020).
- [71] Wei-Ming Huang and Wei-Min Zhang, Nonperturbative renormalization of quantum thermodynamics from weak to strong couplings, *Phys. Rev. Research* **4**, 023141 (2022).
- [72] M. F. Santos and A. R. R. Carvalho, Observing different quantum trajectories in cavity QED, *EPL* **94** 64003 (2011).
- [73] C. Elouard, N. K. Bernardes, A. R. R. Carvalho, M. F. Santos and A. Auffèves, Probing quantum fluctuation theorems in engineered reservoirs, *New J. Phys.* **19** 103011 (2017).
- [74] F. Tacchino, A. Auffèves, M. F. Santos and D. Gerace, Steady State Entanglement beyond Thermal Limits, *Phys. Rev. Lett.*, **120**, 063604 (2018).
- [75] A. E. Allahverdyan, R. Balian, and Th. M. Nieuwenhuizen, Maximal work extraction from finite quantum systems, *Europhys. Lett.* **67**, 565 (2004).
- [76] W. Pusz and S. L. Woronowicz, Passive states and KMS states for general quantum systems, *Commun. Math. Phys.* **58**, 273 (1978).
- [77] T. F. F. Santos, F. Tacchino, D. Gerace, M. Campisi and M. F. Santos, Maximally efficient quantum thermal machines fueled by nonequilibrium steady states, *Phys. Rev. A* **103**, 062225 (2021).
- [78] Correa, L., Palao, J., Alonso, D. et al. Quantum-enhanced absorption refrigerators. *Sci Rep* **4**, 3949 (2014).
- [79] M. Kilgour and D. Segal, Coherence and decoherence in quantum absorption refrigerators, *Phys. Rev. E* **98**, 012117 (2018).
- [80] V. Singh, T. Pandit, and R. S. Johal, Optimal performance of a three-level quantum refrigerator, *Phys. Rev. E* **101**, 062121 (2020).
- [81] F. Ivander, N. Anto-Sztrikacs, and D. Segal, Strong system-bath coupling effects in quantum absorption refrigerators, *Phys. Rev. E* **105**, 034112 (2022).